ORGANOMETALLICS
Article

Organometallics **XXXX,** *XXX,* 000–000 A
DOI: 10.1021/om900980a

Cyclopentadienyl Molybdenum(II/VI) N-Heterocyclic Carbene Complexes: Synthesis, Structure, and Reactivity under Oxidative Conditions

Shenyu Li,[†] Choon Wee Kee,[†] Kuo-Wei Huang,[‡] T. S. Andy Hor,*[,†] and Jin Zhao*[,†,§]

[†]*Department of Chemistry, National University of Singapore, 3 Science Drive 3, 117543, Singapore,* [‡]*KAUST Catalysis Center and Division of Chemical and Life Sciences and Engineering, King Abdullah University of Science and Technology, Thuwal 23955-6900, Kingdom of Saudi Arabia, and* [§]*German Institute of Science and Technology-TUM Asia Pte. Ltd., 10 Central Exchange Green, #03-01, Pixel Building, 138649, Singapore*

Received November 10, 2009

A series of N-heterocyclic carbene (NHC) complexes $CpMo(CO)_2(NHC)X$ (NHC = IMe = 1,3-dimethylimidazol-2-ylidene, X = Br, **1**; NHC = 1,3-dipropylimidazol-2-ylidene, X = Br, **2**; NHC = IMes = 1,3-bis(2,4,6-trimethylphenyl)imidazol-2-ylidene, X = Br, **3**; NHC = IBz = 1,3-dibenzylimidazol-2-ylidene, X = Br, **4a**, and X = Cl, **4b**; NHC = 1-methyl-3-propylimidazol-2-ylidene, X = Br, **5**) and $[CpMo(CO)_2(IMes)(CH_3CN)][BF_4]$ (**6**) have been synthesized and fully characterized. The stability of metal−NHC ligand bonds in these compounds under oxidative conditions has been investigated. The thermally stable Mo(VI) dioxo NHC complex $[CpMoO_2(IMes)][BF_4]$ (**9**) has been isolated by the oxidation of the ionic complex **6** by TBHP (*tert*-butyl hydrogen peroxide). Complex **6** can be applied as a very active (TOFs up to 3400 h^{-1}) and selective olefin epoxidation catalyst. While under oxidative conditions (in the presence of TBHP), compounds **1**−**5** decompose into imidazolium bromide and imidazolium polyoxomolybdate. The formation of polyoxomolybdate as oxidation products had not been observed in a similar epoxidation catalyzed by Mo(II) and Mo(VI) complexes. DFT studies suggest that the presence of Br^- destabilizes the CpMo(VI) oxo NHC carbene species, consistent with the experimental observations.

Introduction

N-Heterocyclic carbenes (NHCs) have been widely used as phosphine alternatives as spectator ligands in the application of transition metal complex catalyzed reactions, such as C−C/C−N coupling, olefin metathesis, and hydrogenation.[1] One of the advantages of NHC ligands over phosphines is the better oxidation resistance.[2] Some NHC complexes show extraordinary stability toward strong oxidizing agents such as peroxodisulfate, which makes it possible to use them in catalytic processes.[3] A variety of catalytic oxidation reactions have been studied using NHC complexes, such as O_2/CO fixation, the oxidation of alcohols, alkyne oxidation, and the oxidation of terminal olefins to ketone, and most of the work in this area was conducted with palladium catalysts.[4] Recently, a Mn(III) complex with a tetradentate NHC ligand was reported and applied as a catalyst for the epoxidation of styrene using PhIO as oxidant to give styrene oxide, suggesting the formation of Mn^{IV}=O and Mn^{V}=O NHC intermediates during the oxygen transfer reactions. However, no spectroscopic evidence of the $Mn^{IV/V}$=O NHC species was given in this work.[5]

In view of the excellent catalytic activities shown in cyclopentadienyl Mo(II) carbonyl complexes, such as $CpMo(CO)_3Cl$ and $CpMo(CO)_3(CH_3)$, in the olefin epoxidation reaction with TBHP (*tert*-butyl hydrogen peroxide) as oxidant,[6,7] and potentially high oxidation resistance of NHC ligands, we are interested in the application of cyclopentadienyl molybdenum carbonyl N-heterocyclic carbene

*Corresponding authors. E-mail: chmzhaoj@nus.edu.sg; andyhor@nus.edu.sg.

(1) See recent reviews: (a) Lin, J. C.Y.; Huang, R. T. W.; Lee., C. S.; Bhattacharyya, A.; Hwang, W. S.; Lin, I. J. B. *Chem. Rev.* **2009**, *109*, 3561. (b) Jacobsen, H.; Correa, A.; Poater, A.; Costabile, C.; Cavallo, L. *Coord. Chem. Rev.* **2009**, *253*, 687. (c) Samojlowicz, C.; Bieniek, M.; Grela, K. *Chem. Rev.* **2009**, *109*, 3708. (d) Marion, N.; Nolan, S. P. *Acc. Chem. Res.* **2008**, *41*, 1440.

(2) Jafarpour, L.; Nolan, S. P. *Adv. Organomet. Chem.* **2000**, *46*, 181.

(3) (a) Muehlhofer, M.; Strassner, T.; Herrmann, W. A. *Angew. Chem., Int. Ed.* **2002**, *41*, 1745. (b) Ahrens, S.; Herdtweck, E.; Goutal, S.; Strassner, T. *Eur. J. Inorg. Chem.* **2006**, 1268. (c) Muehlhofer, M.; Strassner, T.; Herdtweck, E.; Herrmann, W. A. *J. Organomet. Chem.* **2002**, *660*, 121.

(4) Strassner, T. *Top. Organomet. Chem.* **2007**, *22*, 125, and references therein.

(5) Yagyu, T.; Yano, K.; Kimata, T.; Jitsukawa, K. *Organometallics* **2009**, *28*, 2342.

(6) (a) Abrantes, M.; Santos, A. M.; Mink, J.; Kühn, F. E.; Romao, C. C. *Organometallics* **2003**, *22*, 2112. (b) Martins, A. M.; Romao, C. C.; Abrantes, M.; Azevedo, M. C.; Cui, J.; Dias, A. R.; Duarte, M. T.; Lemos, M. A.; Lourenco, T.; Poli, R. *Organometallics* **2005**, *24*, 2582. (c) Al-Ajlouni, A. M.; Veljanovski, D.; Capape, A.; Zhao, J.; Herdtweck, E.; Calhorda, M. J.; Kühn, F. E. *Organometallics* **2009**, *28*, 639.

(7) (a) Zhao, J.; Santos, A. M.; Herdtwerk, E.; Kühn, F. E. *J. Mol. Catal. A: Chem.* **2004**, *222*, 265. (b) Zhao, J.; Sakthivel, A.; Santos, A. M.; Kühn, F. E. *Inorg. Chim. Acta* **2005**, *358*, 4201. (c) Zhao, J.; Herdtweck, E.; Kühn, F. E. *J. Organomet. Chem.* **2006**, *691*, 2199. (d) Zhao, J.; Jain, K. R.; Herdtweck, E.; Kühn, F. E. *Dalton Trans.* **2007**, 5567. (e) Abrantes, M.; Sakthivel, A.; Romao, C. C.; Kühn, F. E. *J. Organomet. Chem.* **2006**, *691*, 3137. (f) Abrantes, M.; Paz, F. A. A.; Valente, A. A.; Pereira, C. C. L.; Gago, S.; Rodrigues, A. E.; Klinowski, J.; Pillinger, M.; Goncalves, I. S. *J. Organomet. Chem.* **2009**, *694*, 1826.

complexes in olefin epoxidations. This system could provide an avenue to introduce chiral NHC ligands to the [$CpMo(CO)_n$] core as a possible route to develop active chiral catalysts for asymmetric epoxidation in which many systems such as Mo(II), Mo(VI), and Re(VII) have failed.[7c−f,8] Compounds $CpM(CO)_2$(IMes)H and [$CpM(CO)_2$(IMes)][$B(C_6F_5)_4$] (M = Mo, W; IMes = 1,3-bis(2,4,6-trimethylphenyl)imidazol-2-ylidene) have been synthesized and employed in catalytic ketone hydrogenation reactions.[9] During the preparation of this paper, some Mo(II) complexes containing *ansa*-bridged cyclopentadienyl-functionalized NHC complexes, (Cp^x-NHC)$Mo(CO)_2I$ (Cp^x = Cp, Cp*, and Cp^{Bz}), have been reported.[10] These complexes, however, are much less active compared to $CpMo(CO)_3X$ (X = Cl or CH_3) toward olefin epoxidation.

It has been reported that some NHC complexes can undergo decomposition through different reaction routes, such as reductive elimination, decomplexation or displacement by competing ligands.[11] Although some metal NHC complexes have been applied for the catalytic oxidation reactions as discussed above, the questions whether NHC metal complexes can be widely used as catalysts for the oxidation reactions and whether metal−NHC ligand bonds are stable under strong oxidative conditions have not been addressed. In order to search for metal NHC complexes with high catalytic activities toward olefin epoxidations and to understand the stability of the metal−NHC ligand bonds under oxidative conditions, we herein report the synthesis and structure of a series of neutral NHC complexes $CpMo(CO)_2$(NHC)X (NHC = IMe = 1,3-dimethylimidazol-2-ylidene, X = Br, **1**; NHC = 1,3-dipropylimidazol-2-ylidene, X = Br, **2**; NHC = IMes = 1,3-bis(2,4,6-trimethylphenyl)imidazol-2-ylidene, X = Br, **3**; NHC = IBz = 1,3-dibenzylimidazol-2-ylidene, X = Br, **4a**, and X = Cl, **4b**; NHC = 1-methyl-3-propylimidazol-2-ylidene, X = Br, **5**) and the ionic complex [$CpMo(CO)_2$(IMes)(CH_3CN)][BF_4] (**6**) and their applications in olefin epoxidations. Their reactivities toward TBHP were studied by NMR, ESI-MS, and DFT calculations. We also report the isolation and characterization of a thermally stable Mo(VI) dioxo complex, [$CpMoO_2$(IMes)][BF_4] (**9**), obtained from the oxidation of **6** by TBHP.

Results and Discussion

Synthesis and Characterization of Compounds 1−5. Compounds $CpMo(CO)_2$(NHC)X (X = Cl, Br) (**1**−**5**) (see Scheme 1) were conveniently synthesized using a transmetalation route by refluxing $CpMo(CO)_3Br$ with silver carbene formed *in situ* in toluene for 40 min. **1**−**5** could also be prepared, albeit in lower yields, using a similar method from $CpMo(CO)_2PPh_3Br$. A mixture of the chloride and bromide forms of **4**, i.e., $CpMo(CO)_2$(NHC)X (X = Br (**4a**) and Cl (**4b**)) is obtained from $CpMo(CO)_2LCl$ (L = CO, PPh_3) and imidazolium bromide. Compounds **1**−**5** were isolated as purple crystals and purified by column chromatography. No further attempt was made to improve the yields. They show good stability at room temperature in both the solid state and solution. They can be handled in laboratory atmosphere and kept under air without decomposition.

Scheme 1

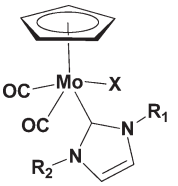

1. X = Br, R_1=R_2=Me
2. X = Br, R_1=R_2=^{n}Pr
3. X = Br, R_1=R_2=Mes
4a. X = Br, R_1=R_2=Bz
4b. X = Cl, R_1=R_2=Bz
5. X = Br, R_1=Me, R_2=^{n}Pr

Scheme 2

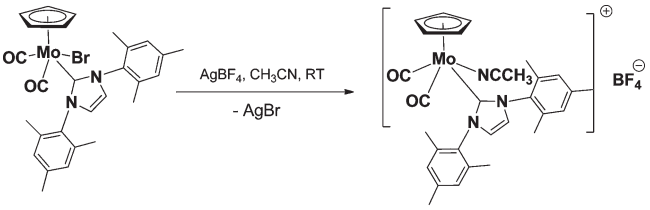

3 **6**

The composition and structure of compounds **1**−**5** were determined by elemental analysis, IR and NMR spectroscopy (^1H, ^{13}C), and X-ray single-crystal diffraction (see discussion below). For all compounds **1**−**5**, in CD_3CN or $CDCl_3$ the ^{13}C NMR signal of the Cp ring appears at δ 95−97 ppm and the ^{13}C NMR signal of the carbene carbon appears at δ 183−190 ppm. The inequivalence of the two carbonyls (δ 254−256/247−252 ppm) at room temperature suggests that they are *cis* oriented and the metal center is chiral. Such inequivalence has been observed for $CpW(CO)_2$(IMes)H and [$CpW(CO)_2$(IMes)(H_2)][$B(C_6F_5)_4$] at −100 °C and for the adduct of [$CpW(CO)_2$(IMes)]-[$B(C_6F_5)_4$] with Et_2CHOH at −40 °C.[9b] For compounds **2**, **4a**, **4b**, and **5**, the ^1H NMR spectra of the methylene protons adjacent to the N atom show an AB-type quartet.[12] In compound **3**, the methyl groups at the phenyl rings of the two sides of the IMes ligand exhibit three discrete singlets in the ^1H NMR (6H each) spectra at room temperature owing to the inequivalence of the methyl groups upon coordination. The IR spectra of compounds **1**−**5** in the solid state exhibit ν_{sym}(CO) at ca. 1950 cm^{-1} and ν_{asym}(CO) at ca. 1860 cm^{-1}. The experimentally measured value of I_{asym}/I_{sym} also indicates that the two CO ligands are *cis* to each other.

Synthesis and Characterization of Compound 6. The ionic complex [$CpMo(CO)_2$(IMes)(CH_3CN)][BF_4] (**6**) was synthesized by the reaction between $CpMo(CO)_2$(IMes)Br (**3**) and $AgBF_4$ in acetonitrile at room temperature (see Scheme 2).

Compound **6** is less stable than compounds **1**−**5**, and it decomposes under laboratory atmosphere after a day. The ^1H NMR signal of Cp ligand of **6** in CD_3CN shifts to lower field compared with that of the neutral analogue **3**. Like **1**−**5**, both the ^{13}C NMR and the IR spectra of **6** indicate that two CO ligands are *cis* oriented. One acetonitrile molecule coordinates to the metal center according to NMR and the elemental analysis as well as X-ray single-crystal diffraction (see discussion below). The positive mode ESI spectrum of **6** shows one set of intense peaks at m/z 517−527 corresponding to [$CpMo(CO)_2$(IMes)]$^+$ and two sets of weak peaks at m/z 461−471 and 489−499 assigned to species

(8) Kühn, F. E.; Zhao, J.; Herrmann, W. A. *Tetrahedron: Asymmetry* **2005**, *16*, 3469, and references therein.
(9) (a) Dioumaev, V. K.; Szalda, D. J.; Hanson, J.; Franz, J. A.; Bullock, R. M. *Chem. Commun.* **2003**, 1670. (b) Wu, F.; Dioumaev, V. K.; Szalda, D. J.; Hanson, J.; Bullock, R. M. *Organometallics* **2007**, *26*, 5079.
(10) Kandepi, V. V. K. M.; Pontes da Costa, A.; Peris, E.; Royo, B. *Organometallics* **2009**, *28*, 4544.
(11) (a) Crudden, C. M.; Allen, D. P. *Coord. Chem. Rev.* **2004**, *248*, 2247. (b) Cavell, K. J.; McGuinness, D. S. *Coord. Chem. Rev.* **2004**, *248*, 671. (c) Cavell, K. J. *Dalton Trans.* **2008**, 6676.
(12) (a) Byabartta, P.; Laguna, M. *Transition Met. Chem.* **2007**, *32*, 180. (b) Lunazzi, L.; Mancinelli, M.; Mazzanti, A. *J. Org. Chem.* **2008**, *73*, 5354.

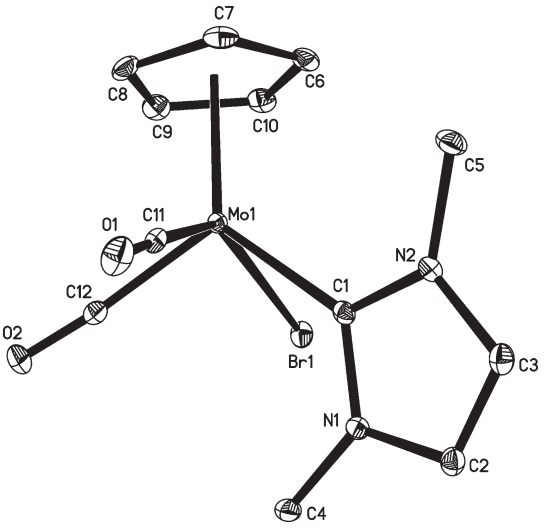

Figure 1. ORTEP diagram of compound **1** (30% probability ellipsoids). Hydrogen atoms are omitted. Selected bond lengths (Å) and angles (deg): Mo(1)−C(12) 1.941(3), Mo(1)−C(11) 1.977(3), Mo(1)−C(1) 2.224(3), C(12)−Mo(1)−C(11) 77.45(11), C(12)−Mo(1)−C(1) 109.61(10), C(11)−Mo(1)−C(1) 70.77(10), N(2)−C(1)−N(1) 103.5(2), N(2)−C(1)−Mo(1) 128.10(18), N(1)−C(1)−Mo(1) 128.26(18).

$[CpMo(IMes)]^+$ and $[CpMo(CO)(IMes)]^+$, respectively, whose isotopic distribution patterns agree with the simulation. $[BF_4]^-$ was observed in the negative mode ESI spectrum as two peaks at m/z 86 and 87 with a characteristic isotopic pattern of the element B.

Molecular Structure of Compounds 1, 2, 3, 4b, 5, and 6 Determined by Single-Crystal X-ray Diffraction. The single crystals of compounds **1**, **2**, **3**, **4b**, and **5** were obtained from a mixture of hexane and ethyl acetate at −19 °C. The single crystal of compound **6** was obtained from a mixture of acetonitrile and ethyl ether at room temperature. Their solid-state structures are shown in Figures 1−6 with selected bond lengths and angles. The molecular structures reveal the characteristic four-legged piano stool arrangement of half-sandwich Mo(II) complexes. In agreement with the IR and NMR data, in all six compounds, two carbonyls are in *cis* configuration and the CO−Mo−CO bond angles are between 76° and 78°. In the ionic compound **6**, one acetonitrile coordinates to the Mo center with a Mo−N distance of 2.172(2) Å. The Mo−C(carbene) bond lengths in **1**−**6** are longer than those reported with similar structure, such as $CpMo(CO)_2(IMes)H$ (2.187(8) Å)[9b] and (Cp*-NHC)-$Mo(CO)_2I$ (Cp*-NHC = η^5-C_4Me_4-CH_2-CHPh-NHC^{Me}) (2.207(3) Å).[10] The Mo−C(carbene) bonds are also slightly longer in **2**, **3**, and **6** (2.24−2.25 Å) than those in compounds **1**, **4b**, and **5** (ca. 2.22 Å). The NHC ligand is coordinated symmetrically, as indicated by very similar angles of N−C−Mo in compounds **1**, **2**, **3**, **4b**, and **6**. In **5**, the angles are somewhat distorted perhaps attributed to the different R substituents in the NHC ligand.

Application of Compounds 1−6 and $CpMo(CO)_3Br$ in Epoxidation Catalysis. Complexes **1**−**6** have been examined as catalysts for the epoxidation of cyclooctene with TBHP in comparison with complexes $CpMo(CO)_3Cl$[6a] and $CpMo(CO)_3(CH_3)$.[7a] Due to the lack of catalytic data of $CpMo(CO)_3Br$ in the literature, the catalytic activity of $CpMo(CO)_3Br$ has also been examined in this work. The time-dependent curves for all catalytic reactions are shown in Figure 7. There was no significant formation of byproduct (e.g., diol). Controlled reactions without catalyst showed no significant formation of the epoxide product. The epoxide yields after 4, 8, and 24 h of reaction time using **1**−**6** as catalysts are shown in Figure 8.

Complex $CpMo(CO)_3Br$ and compound **6** show similarly high activities toward olefin epoxidation to complexes $CpMo(CO)_3Cl$ and $CpMo(CO)_3(CH_3)$ (Figure 7). With a 0.1 mol % catalyst loading, the TOF (turnover frequency)

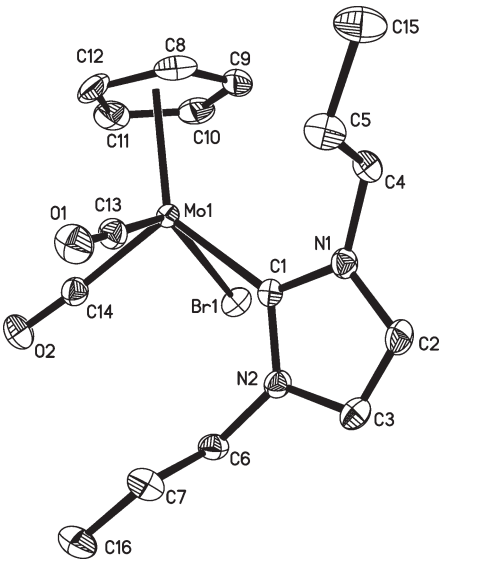

Figure 2. ORTEP diagram of compound **2** (30% probability ellipsoids). Hydrogen atoms are omitted. Selected bond lengths (Å) and angles (deg): C(13)−Mo(1) 1.943(4), Mo(1)−C(14) 1.934(3), Mo(1)−C(1) 2.241(3), C(14)−Mo(1)−C(13) 78.21(13), C(14)−Mo(1)−C(1) 108.12(11), C(13)−Mo(1)−C(1) 75.02(12), N(1)−C(1)−N(2) 103.3(2), N(1)−C(1)−Mo(1) 129.45(19), N(2)−C(1)−Mo(1) 127.24(18).

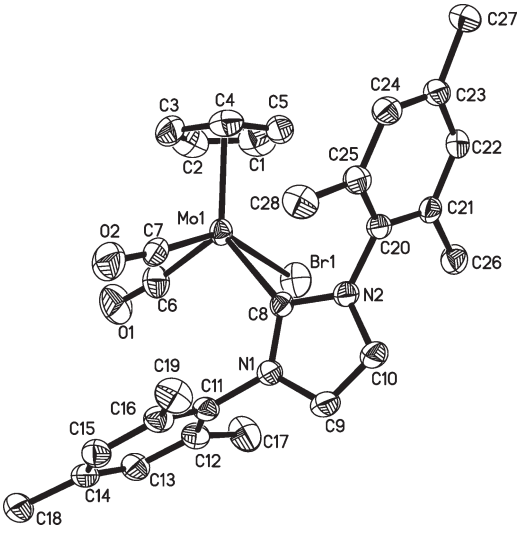

Figure 3. ORTEP diagram of compound **3** (30% probability ellipsoids). Hydrogen atoms are omitted. Selected bond lengths (Å) and angles (deg): Mo(1)−C(6) 1.932(4), Mo(1)−C(7) 1.939(5), Mo(1)−C(8) 2.244(3), C(6)−Mo(1)−C(7) 76.6(2), C(7)−Mo(1)−C(8) 79.15(16), C(6)−Mo(1)−C(8) 107.24(14), N(1)−C(8)−N(2) 102.8(2), N(1)−C(8)−Mo(1) 129.55(19), N(2)−C(8)−Mo(1) 127.6(2).

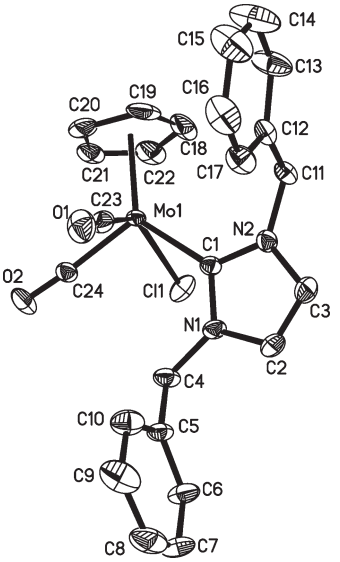

Figure 4. ORTEP diagram of compound **4b** (30% probability ellipsoids). Hydrogen atoms are omitted. Selected bond lengths (Å) and angles (deg): Mo(1)−C(24) 1.924(3), Mo(1)−C(23) 1.984(5), Mo(1)−C(1) 2.221(3), C(24)−Mo(1)−C(23) 78.22(15), C(24)−Mo(1)−C(1) 109.47(13), C(23)−Mo(1)−C(1) 73.38(14), N(2)−C(1)−N(1) 103.3(3), N(2)−C(1)−Mo(1) 129.3(2), N(1)−C(1)−Mo(1) 127.4(2).

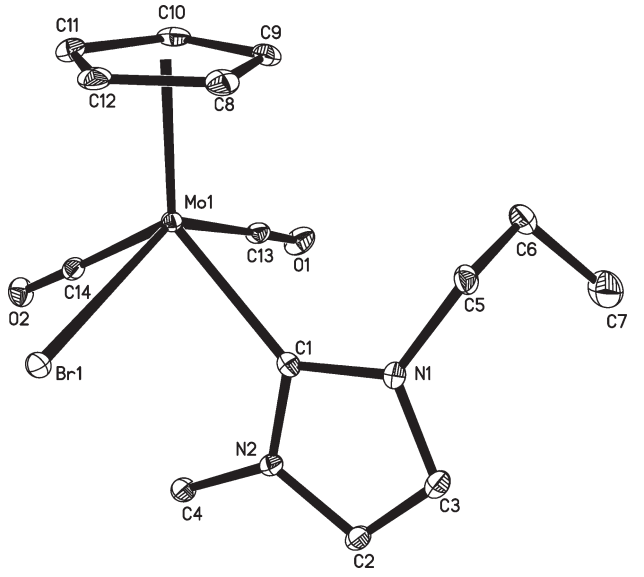

Figure 5. ORTEP diagram of compound **5** (30% probability ellipsoids). Hydrogen atoms are omitted. Selected bond lengths (Å) and angles (deg): Mo(1)−C(14) 1.948(2), Mo(1)−C(13) 1.973(2), Mo(1)−C(1) 2.224(2), C(14)−Mo(1)−C(13) 76.26(8), C(14)−Mo(1)−C(1) 105.13(7), C(13)−Mo(1)−C(1) 72.84(7), N(2)−C(1)−N(1) 103.38(15), N(2)−C(1)−Mo(1) 125.59(13), N(1)−C(1)−Mo(1) 131.02(13).

of compound **6** reaches 3420 h^{-1}, which is higher than that of $CpMo(CO)_3Br$ (2040 h^{-1}). Under similar conditions, $CpMoO_2Cl$-catalyzed oxidations reach maximum TOFs of ca. 4000 h^{-1}.[6a] Compounds **1**−**5** show much lower catalytic activities, although they still appear to be higher than the *ansa*-bridged cyclopentadienyl-functionalized NHC complexes (Cp^x-NHC)$Mo(CO)_2I$ (Cp^x = Cp, Cp*), which give negligible epoxide yields after 5 h.[10] In general, the activities

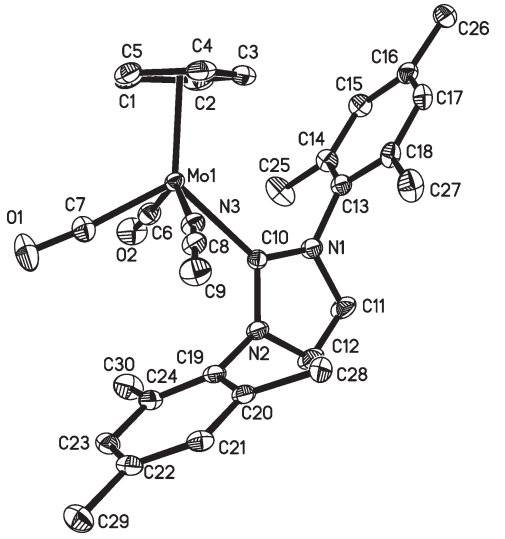

Figure 6. ORTEP diagram of the cation of $[CpMo(CO)_2(IMes)(CH_3CN)]^+$ in compound **6** (30% probability ellipsoids). Hydrogen atoms are omitted. Selected bond lengths (Å) and angles (deg): Mo(1)−C(6) 1.996(3), Mo(1)−C(7) 1.947(3), Mo(1)−C(10) 2.249(3), Mo(1)−N(3) 2.172(2), C(6)−Mo(1)−C(7) 75.97(13), C(6)−Mo(1)−C(10) 75.75(11), C(7)−Mo(1)−C(10) 110.34(12), N(1)−C(10)−N(2) 102.7(2), N(1)−C(10)−Mo(1) 128.0(2), N(2)−C(10)−Mo(1) 128.6(2).

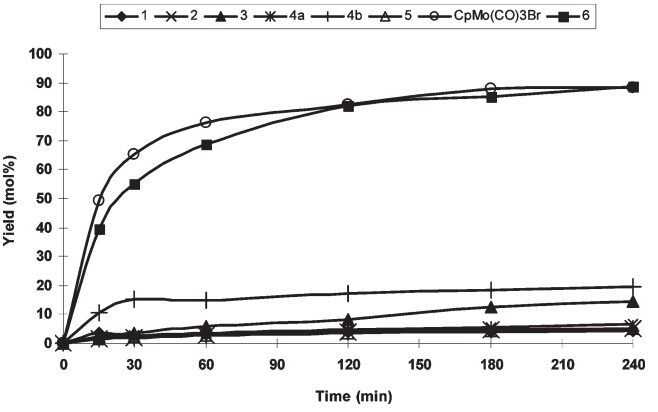

Figure 7. Time-dependent yields of cyclooctene epoxide using compounds **1**−**6** and $CpMo(CO)_3Br$ as catalysts and using TBHP as oxidant at 55 °C (catalyst:substrate:oxidant = 1:100:200).

observed are almost independent of the NHC ligands present in **1**−**5**, although among them, **3** and **4b** are slightly more active (Figure 7). During the course of reactions using **1**−**5** as catalysts, formation of pale yellow or white precipitates was observed (the characterization of which is discussed below). This suggests that **1**−**5** decompose during the oxidation reaction, and the decomposition products are poorly active toward epoxidation.

Stability of the Metal−NHC Ligand Bond in $CpMo(CO)_2$(NHC)X under Oxidative Conditions. The significant difference in the catalytic activity between the neutral complexes **1**−**5** and the ionic complex **6** prompted us to investigate the stability of the metal−NHC ligand bond of these NHC complexes under the oxidative conditions (in the presence of TBHP) by using ^{1}H NMR and ESI-MS.

Stability of Mo−C_{NHC} Bonds in 3 and 4a under Oxidative Conditions. Kinetic ^{1}H NMR experiments on the oxidation reactions of **3** and **4a** were carried out by treatment with a

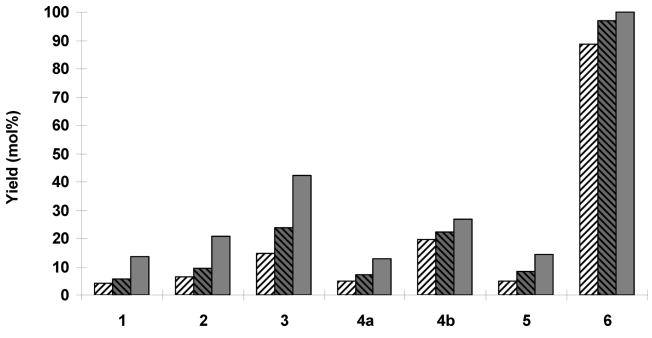

Figure 8. Yields of the cyclooctene epoxide after 4 h (hatched bars), 8 h (gray and hatched bars), and 24 h (gray bars) of reaction time using the compounds **1**−**6** as catalysts in the presence of TBHP at 55 °C (catalyst:substrate:oxidant = 1:100:200).

5-fold excess of TBHP (~5.5 M in decane over molecular sieves 4 Å) at room temperature in CD_3CN upon stirring of the mixtures. In the case of **4a**, the purple color persisted for 15 min; then a fast change from purple to yellow occurred and a pale yellow precipitate was formed. The Cp resonance at δ 5.44 ppm in the ^{1}H NMR spectrum disappeared completely after 15 min of reaction. A single signal at δ 6.56 ppm and a set of weak peaks at δ 6.43−6.26 ppm were observed. The characteristic signals of an imidazolium salt appeared at δ 7.41−7.43 (12H), 5.39 (4H), and 9.19 ppm (1H). After 20 min, besides the peaks from the imdazolium salt, only a set of very weak peaks at δ 6.54, 6.45, and 6.36 ppm could be observed. Similar observations were noted in **3**. After 15 min, the characteristic signals of the corresponding imidazolium salt appeared at δ 8.79 (1H), 7.76 (2H), 7.14 (4H), 2.36 (6H), and 2.12 ppm (12H). The peaks at δ 6.54−6.26 ppm are likely from the decomposition products of the Cp ligand.

By comparing the ^{1}H NMR spectra of the corresponding imidazolium bromides in CD_3CN, there is a shift of the signal of the proton of NC*H*N in the ^{1}H NMR of the imidazolium salt formed from the reaction between **3** or **4a** and TBHP. This difference may be due to the presence of the excess amount of TBHP and ^{t}BuOH formed during the oxidation reaction. It was confirmed by treating the NMR sample of IBzHBr in CD_3CN with 0.05 mL of TBHP. It was observed that the signal of NC*H*N shifted from δ 9.29 to δ 9.15 ppm. Similarly, in the case of IMesHBr, the signal of NC*H*N shifted from δ 9.18 to δ 8.87 ppm after TBHP was added. As was observed in the kinetic reactions discussed above, a broad peak at *ca.* δ 9 ppm is due to the presence of TBHP. The imidazolium salt formed from the oxidation reactions is accordingly assigned as imidazolium bromide.

The pale yellow precipitate formed during the oxidation reactions using **3** as catalyst was found to be soluble in DMSO. It was characterized by IR, ^{1}H NMR, ESI-MS, and elemental analysis (see Experimental Section). The IR spectrum shows strong absorptions at 955 and 800 cm^{-1} from the Mo═O bond stretching. The proton NMR spectrum shows that the obtained solid is a pure imidazolium salt with the most characteristic singlet peak at δ 9.63 ppm. In order to identify the anion, ESI-MS analysis was performed. The imidazolium cation can be observed (m/z 305.3) in the positive mode spectrum. The negative mode spectrum reveals seven Mo-containing anionic species including $\{[IMesH][Mo_6O_{19}]\}^-$ centered at m/z 1183, $[HMo_6O_{19}]^-$, $[Mo_6O_{19}]^{2-}$, $[Mo_5O_{16}]^{2-}$, $[Mo_4O_{13}]^{2-}$, $[Mo_3O_{10}]^{2-}$, and $[HMoO_4]^-$, which are assigned on the basis of the m/z values, the difference in m/z between adjacent peaks and their isotopic distribution patterns (see Figure 9). Combining the spectroscopic results and the elemental analysis data, the pale yellow precipitate is identified as $[IMesH]_2[Mo_6O_{19}]$. The formation of polyoxomolydates as anion in metal complexes has been reported in the literature. For example, a reaction of $MoO_2(S_2CNMe_2)$ with $RuCl_3 \cdot xH_2O$ in acetone at reflux afforded a Ru complex with $[Mo_6O_{19}]$ as anion.[13a] Reactions of $MoO_2(acac)_2$ with corresponding ligands (L) in aqueous methanol have been reported to give complexes $[Mo_2O_5L_6][Mo_6O_{19}]$ (L = H_2O, dimethylformamide, etc.).[13b] However, the polyoxomolydate species as oxidation products have not been characterized in the similar epoxidation reactions catalyzed by Mo(II) and Mo(VI) complexes in the presence of TBHP or H_2O_2, although in some cases a white precipitate could be observed in the epoxidation catalysis under similar conditions.[6c] In our system, the formation of polyoxomolydates may be due to the presence of trace amounts of water in the oxidation system. The catalytic activity of $[IMesH]_2[Mo_6O_{19}]$ was examined in this work, and it was found that under the same catalytic conditions it shows similar activity to compound **3**.

ESI-MS analysis was carried out to follow the reaction between TBHP and **4a** (ratio 10:1) in acetonitrile at room temperature. Initially, the positive mode ESI spectrum of **4a** (Figure 10a) showed four sets of peaks centered at m/z 507.5, 467, 439, and 411, corresponding to $[CpMo(CO)_2(IBz)(CH_3CN)]^+$, $[CpMo(CO)_2(IBz)]^+$, $[CpMo(CO)(IBz)]^+$, and $[CpMo(IBz)]^+$, respectively, and MS/MS analysis was performed to verify the presence of these species. After 25 min of reaction time with TBHP, the ESI-MS spectrum indicated the decomposition of **4a** (Figure 10b).

The peaks at m/z 249 and 577 are assigned to $[IBzH]^+$ and **7**, respectively. The assignment of **8** to the peak at m/z 293 is strongly supported by the loss of m/z 44 in the MS/MS coupled with CID (collision-induced dissociation). Its detection suggests that free carbene could be formed during the oxidation of $CpMo(CO)_2(IBz)Br$. This is supported by the well-documented reaction between carbene and CO_2.[14] In our case, CO_2 is generated from the oxidation of $CpMo(CO)_2(IBz)Br$. Both sets of peaks at m/z 349 and 679 can be assigned to imidazolium derivatives on the basis of CID coupled with MS^n and the isotopic distribution; however, their structures could not be interpreted satisfactorily with the current data. In the negative mode spectrum, the set of peaks from Br^- was observed, which supports the presence of imidazolium bromide in the reaction solution. The peaks from $[Mo_6O_{19}]^{2-}$, $[Mo_5O_{16}]^{2-}$, and $[Mo_4O_{13}]^{2-}$ were identified from their characteristic isotopic distribution patterns and m/z ratios.

$[CpMoO_2(IBz)]^+$ species was detected in the reaction mixture of **4a** and TBHP only after 5 min. However, its peaks overlap with those of $[CpMo(CO)(IBz)]^+$, but the isotopic distribution observed is in agreement with the theoretically predicted one based on the combination of both ions (see Figure 11). This is consistent with the observation of a singlet peak in the ^{1}H NMR at δ 6.56 ppm, which could be assigned to the protons of the Cp ring in the $[CpMoO_2(IBz)]^+$ species.

Stability of Mo−C_{NHC} Bond in 6 under Oxidative Conditions and the Isolation of $[CpMoO_2(IMes)][BF_4]$ (9). Oxidation of

(13) (a) Wu, F.-H.; Liu, Y.-L.; Duan, T.; Lu, L.; Zhang, Q.-F.; Leung, W.-H. *Z. Naturforsch. B* **2009**, *64*, 800. (b) Pedrosa, M. R.; Aguado, R.; Díez, V.; Escribano, J.; Sanz, R.; Arnáiz, F. J. *Eur. J. Inorg. Chem.* **2007**, 3952.

(14) (a) Shirley, D. A.; Alley, P. W. *J. Am. Chem. Soc.* **1957**, *79*, 4922. (b) Voutchkova, A. M.; Appelhans, L. N.; Chianese, A. R.; Crabtree, R. H. *J. Am. Chem. Soc.* **2005**, *127*, 17624. (c) Voutchkova, A. M.; Feliz, M.; Clot, E.; Eisenstein, O.; Crabtree, R. H. *J. Am. Chem. Soc.* **2007**, *129*, 12834. (d) Zhou, H.; Zhang, W.-Z.; Liu, C.-H.; Qu, J.-P.; Lu, X.-B. *J. Org. Chem.* **2008**, *73*, 8039.

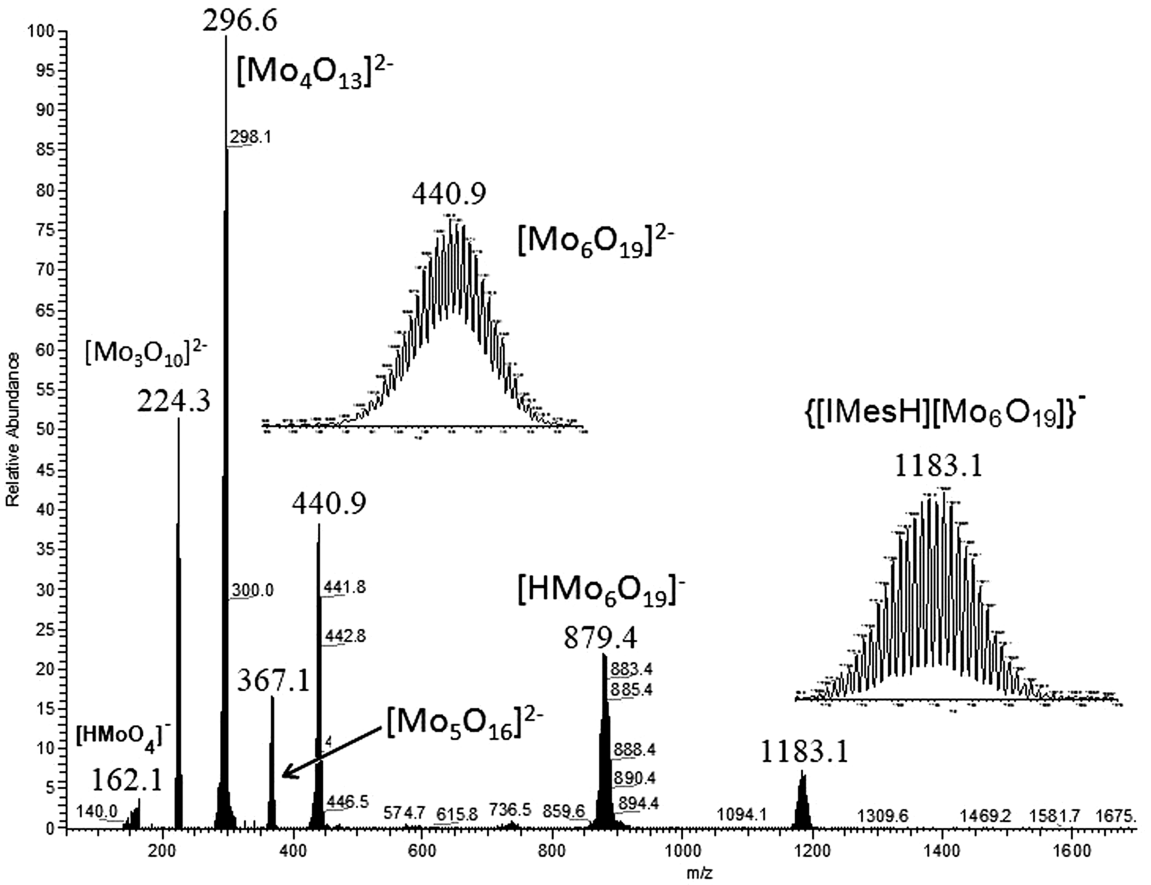

Figure 9. Negative mode ESI-MS spectrum of the imidazolium salt $[Mo_6O_{19}][IMesH]_2$ obtained from the oxidation reaction between **3** and TBHP.

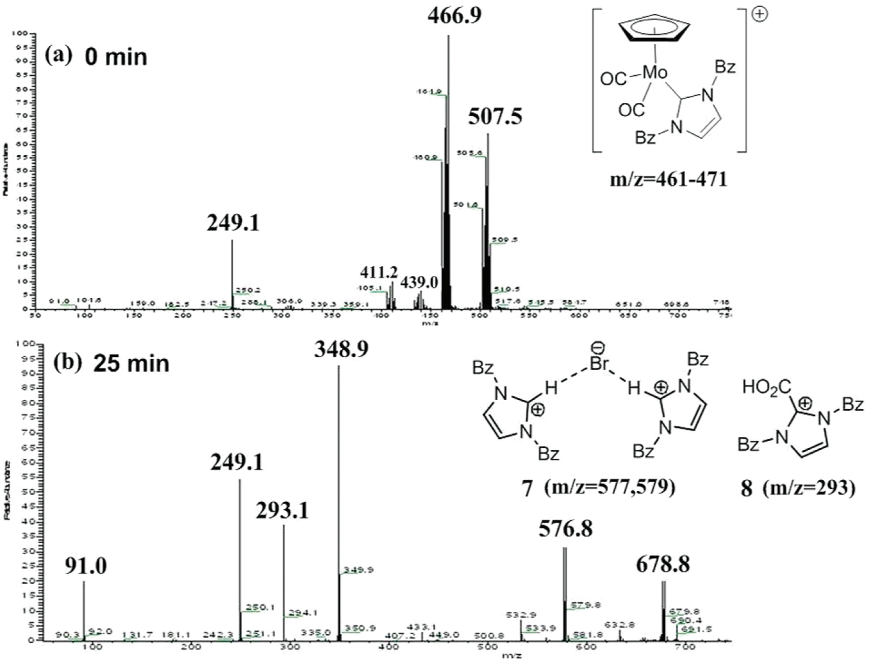

Figure 10. Positive mode ESI-MS spectrum of **4a** (a) and the positive mode ESI-MS spectrum of the reaction mixture of **4a** and TBHP (1:10) after 25 min of reaction time (b).

compound **6** in CH_3CN by TBHP (~5.5 M in decane over molecular sieves 4 Å) gives the dioxo complex $[CpMoO_2(IMes)][BF_4]$ (**9**) (see Scheme 3).

Compound **9** demonstrates relatively high stability compared to previously reported high oxidation state molybdenum NHC complexes obtained from the reactions

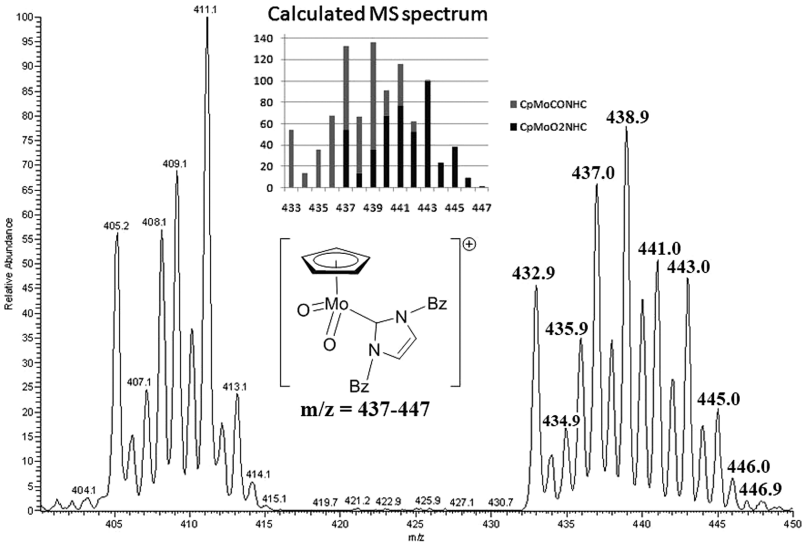

Figure 11. Positive mode ESI-MS spectrum of the reaction mixture of compound **4a** and TBHP (1:10) after 5 min of reaction time.

between $MoO_2Cl_2(THF)_2$ and free NHC ligands.[15] The stability of **9** enabled it to be isolated and fully characterized as a dioxo complex. The formation of **9** was studied by the kinetic ^{1}H NMR experiments through the treatment of **6** with a 5-fold excess of TBHP at room temperature in CD_3CN upon stirring of the mixture in a glovebox under argon (see Figure 12).

After 5 min, three single peaks appeared at δ 6.26, 7.11, and 7.85 ppm, respectively, in a ratio of 5:4:2 due to the formation of **9**. The intensity of these three peaks increased with time, while the intensity of peaks from **6** decreased. After 80 min, the peaks from **9** dominated the spectrum. Comparing with the ^{1}H NMR spectrum of **6**, the signal of the Cp ring in **9** shifts to lower field significantly and the *meta*-CH groups in the two phenyl rings become equivalent, with one single peak appearing at the average chemical shifts of the two nonequivalent *meta*-CH groups in the carbonyl precursor, **6**. Similarly, four *ortho*-methyl groups at the phenyl rings are also equivalent with one single peak, implying a fast rotation of the N−mesityl bond in the IMes ligand. The chemical shift of the CH=CH in the NHC ring does not change significantly. The ^{13}C NMR carbene carbon signal of **9** is shifted to higher field (δ 167 ppm) in comparison with that of low oxidation state complexes **1**−**6** (δ 180−190 ppm). The formation of **9** has also been proved by ESI-MS analysis, IR, and elemental analysis. In the ESI-MS spectrum, the characteristic peaks of $[CpMoO_2(IMes)]^+$ appear at 494−504 *m*/*z*, and peaks of polyoxomolydates are not observed. The IR spectrum shows the strong absorptions at 956 and 801 cm^{-1} from the Mo=O stretching vibration. This work shows that thermally stable ionic Mo(VI) dioxo NHC complex can be formed through the oxidation of the carbonyl precursors. This is similar to the formation of $Cp'MoO_2Cl$ (Cp' = Cp, Cp*, Cp^{Bz}) from $Cp'Mo(CO)_3Cl$.[6a] The high catalytic activity of compound **6** is attributed to the stability of the metal−NHC ligand bond in the $[CpMoO_2(IMes)]^+$ species, which is formed *in situ* in the catalytic epoxidation mixture containing precatalyst **6** and

Scheme 3

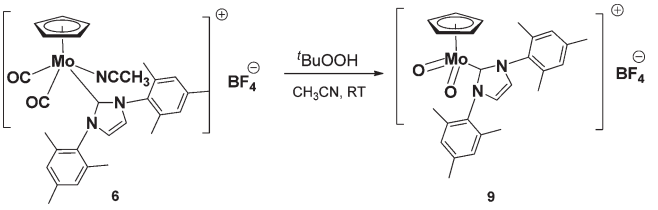

the oxidant TBHP. Under the same conditions, compounds **6** and **9** show very similar catalytic activities toward cyclooctene epoxidation using TBHP as oxidant. These facts support that they are mechanistically related.

DFT Studies. DFT calculations were performed at the B3LYP level of theory[16−18] in order to gain more insight into the difference in the stability of Mo−NHC ligand bonds in the neutral complexes **1**−**5** and the ionic complex **6** under oxidative conditions. Compound **1** was chosen to maximize computational efficiency. Consistent with the X-ray molecular structure, the *trans* isomer (**1**-*trans*) is 8.9 kcal/mol less stable than complex **1**. The geometrical parameters of the fully optimized structure are in general in good agreement with the experimental results, with slightly longer bond distances (Table 1).

(15) (a) Herrmann, W. A.; Lobmaier, G. M.; Elison, M. *J. Organomet. Chem.* **1996**, *520*, 231. (b) Mas-Marzá, E.; Reis, P. M.; Peris, E.; Royo, B. *J. Organomet. Chem.* **2006**, *691*, 2708.

(16) Frisch, M. J.; Trucks, G. W.; Schlegel, H. B.; Scuseria, G. E.; Robb, M. A.; Cheeseman, J. R.; Montgomery, J. A., Jr.; Vreven, T.; Kudin, K. N.; Burant, J. C.; Millam, J. M.; Iyengar, S. S.; Tomasi, J.; Barone, V.; Mennucci, B.; Cossi, M.; Scalmani, G.; Rega, N.; Petersson, G. A.; Nakatsuji, H.; Hada, M.; Ehara, M.; Toyota, K.; Fukuda, R.; Hasegawa, J.; Ishida, M.; Nakajima, T.; Honda, Y.; Kitao, O.; Nakai, H.; Klene, M.; Li, X.; Knox, J. E.; Hratchian, H. P.; Cross, J. B.; Bakken, V.; Adamo, C.; Jaramillo, J.; Gomperts, R.; Stratmann, R. E.; Yazyev, O.; Austin, A. J.; Cammi, R.; Pomelli, C.; Ochterski, J. W.; Ayala, P. Y.; Morokuma, K.; Voth, G. A.; Salvador, P.; Dannenberg, J. J.; Zakrzewski, V. G.; Dapprich, S.; Daniels, A. D.; Strain, M. C.; Farkas, O.; Malick, D. K.; Rabuck, A. D.; Raghavachari, K.; Foresman, J. B.; Ortiz, J. V.; Cui, Q.; Baboul, A. G.; Clifford, S.; Cioslowski, J.; Stefanov, B. B.; Liu, G.; Liashenko, A.; Piskorz, P.; Komaromi, I.; Martin, R. L.; Fox, D. J.; Keith, T.; Al-Laham, M. A.; Peng, C. Y.; Nanayakkara, A.; Challacombe, M.; Gill, P. M. W.; Johnson, B.; Chen, W.; Wong, M. W.; Gonzalez, C.; Pople, J. A. *Gaussian 03, Revision E.01*; Gaussian, Inc.: Wallingford, CT, 2004.

(17) Becke, A. D. *J. Chem. Phys.* **1993**, *98*, 5648.

(18) Lee, C.; Yang, W.; Parr, R. G. *Phys. Rev. B: Condens. Matter* **1988**, *37*, 785.

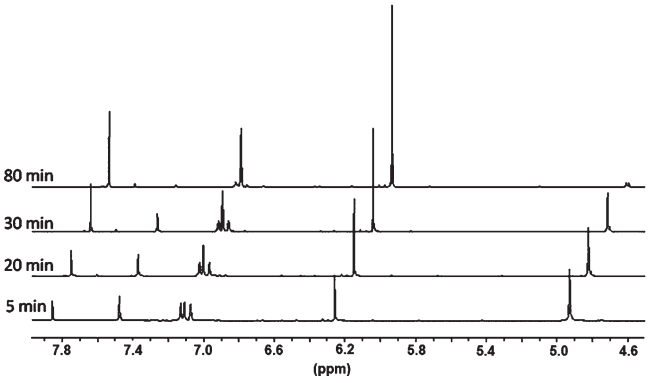

Figure 12. Kinetic ^{1}H NMR experiments on the reaction of compound **6** and TBHP at room temperature in CD_3CN.

Table 1. Calculated Bond Lengths and Angles vs Experimental Data for $CpMo(CO)_2(IMe)Br$ (1)[a]

bond length (Å) or angle (deg)	experimental (X-ray)	calculated
Mo−C1	2.224	2.242
Mo−Br	2.667	2.723
Mo−C11	1.977	1.981
Mo−C12	1.941	1.964
Mo−Cp	2.021	2.097
C1−Mo−Br	80.35	76.10
C11−Mo−C12	77.45	79.09

[a] See Figure 1 for labeling.

Table 2. Calculated Structural Parameters of CpMo(IMe) Complexes

geometrical parameter	$CpMo(CO)_2$-(IMe)Br	$CpMoO_2$-(IMe)Br (*cis*)	$CpMoO_2$-(IMe)Br (*trans*)	$CpMoO_2$-$(IMe)^+$
Mo−Br	2.723	2.931	2.732	
Mo−C(NHC)	2.242	2.254	2.336	2.182
Mo-Cp	2.097	2.233	2.227	2.177
Mo=O		1.745/1.717	1.732/1.729	1.715/1.715

Gas phase geometry optimization of $CpMoO_2(IMe)Br$ was performed using the same method. The *trans* isomer is 1.4 kcal/mol more stable that the *cis* isomer. For both *cis* and *trans* isomers, an increase of the Mo−ligand bond lengths was predicted (Table 2). This result prompted us to investigate the structure of $[CpMoO_2(IMe)]^+$. Overall shortening of Mo=O, Mo−C(NHC), and Mo−Cp bonds was predicted upon removal of Br^- from the coordination sphere (Table 2).

This suggests that the coordination of Br^- to Mo weakens the rest of the Mo−ligand bonds. The plausible destabilizing effect of Br^- was further examined by calculating the IMe binding energies to $[CpMoO_2]^+$ and $CpMoO_2Br$ fragments. It was found that in the gas phase the dissociation of IMe from $[CpMoO_2(IMe)]^+$ is highly thermodynamically disfavored (ΔG = 85.1 kcal/mol). In sharp contrast, the dissociation of IMe from *trans*-$CpMoO_2(IMe)Br$ is exergonic (ΔG = −7.9 kcal/mol). These results suggest that the presence of Br^- may cause the dissociation of the carbene ligands in the oxidation products of compounds **1**−**5**, i.e., $CpMoO_2$-(NHC)Br, leading to the decomposition and deactivation of these Mo-oxo species. To examine this hypothesis, a CD_3CN solution of $[CpMoO_2(IMes)]^+[BF_4]$ (**9**) was treated with one molar equivalent of $^nBu_4NBr$. The ^{1}H NMR indicated that the imidazolium salt was formed in the reaction mixtures and $[CpMoO_2(IMes)][BF_4]$ fully decomposed. It is similar to that of the reaction between $CpMo(CO)_2$-(IMes)Br and TBHP. Furthermore, the formation of the corresponding imidazolium salt and the decomposition of $CpMoO_2Br$ were also observed in the ^{1}H NMR spectra of the reaction mixture when a CD_3CN solution of $CpMoO_2Br$, prepared from the oxidation of $CpMo(CO)_3Br$ solution by TBHP,[6a] was treated with one molar equivalent of free NHC, 1,3-bis(2,6-diisopropylpheny)imidazol-2-ylidene. While the decomposition route of $CpMoO_2$ species into polyoxomolybdates is not clear, these observations together with the calculation results confirm that the presence of Br^- destabilizes the CpMo(VI) oxo NHC carbene species.

Conclusions

In this work, a series of NHC complexes with the formula $CpMo(CO)_2(NHC)X$ (**1**−**5**) and the ionic complex $[CpMo(CO)_2(IMes)(CH_3CN)][BF_4]$ (**6**), as well as the oxidation product $[CpMoO_2(IMes)]^+[BF_4]^-$ (**9**), have been synthesized and fully characterized. Complexes **1**−**5** show low catalytic activities toward the epoxidation of cyclooctene with TBHP, while compound **6** is a highly active catalyst with a high TOF value comparable to compound $CpMo(CO)_3Cl$. Compound **9** can be formed *in situ* in the epoxidation reaction system (using TBHP as oxidant) catalyzed by **6**, and it shows similarly high catalytic activity to its precursor **6**. This is similar to the olefin epoxidation catalyzed by $CpMo(CO)_3Cl$ (using TBHP as oxidant), where $CpMoO_2Cl$ is formed *in situ* in the reaction system. The latter 16*e* complex has been attributed to the actual catalyst species.[6a] For compounds **1**−**5**, the proposed oxidation products are a class of Mo(VI) dioxo compounds with the formula $CpMoO_2$-(NHC)Br; however, these 18*e* complexes cannot be isolated. In our ESI-MS studies, only $[CpMoO_2(NHC)]^+$ species can be observed at the beginning of the reaction between TBHP and $CpMo(CO)_2(NHC)Br$. $CpMoO_2(NHC)Br$ species decompose to imidazolium salts (bromide and polymolybdate) and some unidentified products, which leads to the poor catalytic activities of **1**−**5**. DFT calculations suggest that the presence of Br^- destabilizes the Mo−NHC ligand bond in the CpMo(VI) oxo NHC carbene species. Combined with the experimental observations, the coexistence of Br^- and NHC ligands in $CpMoO_2(NHC)Br$ is responsible for the decomposition of the species with a $CpMoO_2$ core in our system.

The high catalytic activity of the ionic compound **6** shown in the olefin epoxidation reactions with TBHP as oxidant and the stability of the Mo−NHC ligand bond in the oxidation product of **6** are encouraging. This provides a possible route to introduce chiral and/or some functional groups to the $[CpMo(CO)_2(NHC)]^+$ core in order to develop active chiral selective catalysts or heterogenized catalysts for heterogeneous epoxidation reactions.

Experimental Section

General Considerations. All preparations and manipulations were performed using standard Schlenk techniques under a nitrogen atmosphere. Solvents were dried by standard procedures, distilled under nitrogen, and used immediately. TBHP (*tert*-butyl hydrogen peroxide, ~5.5 M in decane over molecular sieves 4 Å or 5.0−6.0 M in decane) was purchased from Sigma-Aldrich. Elemental analyses for C, H, and N were performed on a Perkin-Elmer PE 2400 CHNS elemental analyzer. ^{1}H and ^{13}C

NMR were measured in CD_3CN and $CDCl_3$ at room temperature with an AMX500 500 MHz FT NMR spectrometer. IR spectra were recorded on a Shimadzu IR-470 spectrometer using KBr pellets as IR matrix. ESI-MS was performed on a Finnigan LCQ quadrapole ion trap mass spectrometer. Sample was introduced into the ESI source using a syringe pump. The following ESI-MS parameters were kept constant for all measurements: spray voltage = ±3.5 kV; capillary temperature = 100 °C; flow rate = 5 μL min^{-1}; tube lens offset = 0 V; and capillary voltage = 0 V. The spectra were obtained as an average of at least 20 scans. Catalytic runs were monitored by GC methods on an Agilent 6890 Series GC instrument with a J&W DB-1 column. The preparation of imidazolium bromide[19−22] and that of the corresponding silver NHC complexes[23−25] were based on the literature procedures. $CpMo(CO)_3Br$[26] and $CpMo(CO)_2PPh_3Br$[27] were prepared according to literature methods.

Synthesis of 1,3-Bis(2,4,6-trimethylphenyl)imidazolium Bromide (IMesHBr). To a solution of *N,N′*-bis(2,4,6-trimethylphenyl)ethanediimine[28] (10 mmol) in toluene (20 mL) at 10 °C was added paraformaldehyde (0.3 g, 10 mmol) with vigorously stirring. After 30 min, the solution was cooled to 0 °C, and an aqueous solution of HBF_4 (50% w/v, 10 mmol, 2 g) was added dropwise. The resulting solution was stirred at room temperature for a further 30 min and then heated to 40 °C for 12 h. After cooling to room temperature, diethyl ether (10 mL) was added and the slurry was filtered, washed with ethyl acetate and THF, and vacuum-dried, yielding [IMesH][BF_4] as a beige powder (yield: 3.05 g, 78%). To the suspension of an ethyl acetate solution (10 mL) of $IMesHBF_4$ (1.25 mmol, 0.5 g) was introduced dropwise a saturated acetone solution of $^nBuN_4Br$ (5 mmol, 1.6 g). The mixture was stirred for 12 h at room temperature. The resultant suspension was filtered and washed with ethyl acetate and dried under vacuum, resulting in IMesHBr as a white powder (yield: 0.33 g, 69%).

The ^{1}H NMR data of the imidazolium salts (500 MHz, in CD_3CN):

1,3-Dimethylimidazolium (IMeHBr): δ (ppm) 9.17 (s, 1H, NC*H*N), 7.44 (s, 2H, =C*H*), 3.87 (s, 6H, NCH_3).

1,3-Dipropylimidazolium bromide (I^{n}PrHBr): δ (ppm) 9.55 (s, 1H, NC*H*N), 7.61 (s, 2H, =C*H*), 4.18 (m, 4H, $NCH_2CH_2CH_3$), 1.87−1.82 (m, 4H, $NCH_2CH_2CH_3$), 0.86 (t, 6H, $NCH_2CH_2CH_3$).

1,3-Bis(2,4,6-trimethylphenyl)imidazolium bromide (IMesHBr): δ (ppm) 9.18 (s, 1H, NC*H*N), 7.73 (d, 2H, =C*H*), 7.15 (s, 4H,m-*H*-Mes), 2.36 (s, 6H, *p*-*Me*-Mes), 2.13 (s, 12H, *o*-*Me*-Mes).

1,3-Dibenzylimidazolium bromide (IBzHBr): δ (ppm) 9.29 (br, 1H, NC*H*N), 7.41−7.43 (m, 12H, CH_2Ph and =C*H*), 5.39 (s, 4H, NCH_2Ph)

1-Methyl-3-propyimidazolium bromide (IMe^{n}PrHBr): δ (ppm) 9.43 (s, 1H, NC*H*N), 7.57 (s, 1H, =C*H*), 7.52 (s, 1H, =C*H*), 4.17 (t, 2H, J = 7.5 Hz, $NCH_2CH_2CH_3$), 3.88 (s, 3H, NCH_3), 1.86−1.81 (m, 2H, $NCH_2CH_2CH_3$), 0.86 (t, 3H, $NCH_2CH_2CH_3$).

Synthesis of Compounds 1, 2, 4a, and 5. Ag_2O (1 mmol) was added to a solution of the imidazolium bromide (1 mmol) in CH_2Cl_2 (15 mL). After stirring at room temperature for 24 h (exclusion of light), the reaction mixture was filtered through Celite. The filtrate was dried under vacuum and was dissolved in toluene (20 mL). $CpMo(CO)_3Br$ (0.6 mmol) was then added to the toluene solution. After refluxing for 40 min under stirring, the obtained purple solution was dried under vacuum, and the purple solid was purified by column chromatography eluted by a mixture of hexane and ethyl acetate (2:1 to 5:1) to give the product as a purple solid.

(η^5-C_5H_5)Mo(CO)$_2$(IMe)Br (1). (Yield: 30%.) ^{1}H NMR (500 MHz, CD_3CN): δ (ppm) 7.16 (s, 2H, =C*H*), 5.61 (s, 5H, *Cp*), 3.64 (s, 6H, NCH_3). ^{13}C NMR (125.77 MHz, CD_3CN): δ (ppm) 255.87 (s, Mo-*C*O), 251.80 (s, Mo-*C*O), 185.01 (s, N*C*N), 124.81 (s, =*C*H), 96.04 (s, *Cp*), 40.53 (s, NCH_3). IR (KBr)/cm^{-1}: ν_{sym}(CO) 1955 (vs), ν_{asym}(CO) 1832 (vs), I_{asym}/I_{sym} = 1.06 (predicted OC−Mo−CO angle 92°). Anal. Calcd for $C_{12}H_{13}BrN_2O_2Mo$: C, 36.67; H, 3.33; N, 7.13. Found: C, 36.96; H, 3.32; N, 6.89.

(η^5-C_5H_5)Mo(CO)$_2$(I^{n}Pr)Br (2). (Yield: 30%.) ^{1}H NMR (500 MHz, CD_3CN): δ (ppm) 7.26 (s, 2H, =C*H*), 5.56 (s, 5H, *Cp*), 4.05−4.00 (br m, 2H, $NCH_2CH_2CH_3$), 3.85−3.80 (br m, 2H, $NCH_2CH_2CH_3$),1.81−1.74 (m, 4H, $NCH_2CH_2CH_3$), 0.94 (t, 6H, $NCH_2CH_2CH_3$, J = 7.55 Hz). ^{13}C NMR (125.77 MHz, CD_3CN): δ (ppm) 254.95 (s, Mo-*C*O), 251.19 (s, Mo-*C*O), 183.36 (s, N*C*N), 123.58 (s, =*C*H), 96.23 (s, *Cp*), 54.26 (s, $NCH_2CH_2CH_3$), 24.69 (s, $NCH_2CH_2CH_3$), 11.33 (s, $NCH_2CH_2CH_3$). IR (KBr)/cm^{-1}: ν_{sym}(CO) 1946 (vs), ν_{asym}(CO) 1841 (vs), I_{asym}/I_{sym} = 1.17 (predicted OC−Mo−CO angle 95°). Anal. Calcd for $C_{16}H_{21}BrN_2O_2Mo$: C, 42.78; H, 4.71; N, 6.24. Found: C, 42.70; H, 4.53; N, 6.21.

(η^5-C_5H_5)Mo(CO)$_2$(IBz)Br (4a). (Yield: 50%.) ^{1}H NMR (500 MHz, CD_3CN): δ (ppm) 7.40−7.26 (br m, 10H,CH_2Ph), 7.06 (s, 2H, =C*H*), 5.41 (s, 5H, *Cp*), 5.36−5.23 (q, 4H, NCH_2Ph, J = 15.75 Hz). ^{13}C NMR (125.77 MHz, CD_3CN): δ (ppm) 254.04 (s, Mo-*C*O), 251.22 (s, Mo-*C*O) 186.95 (s, N*C*N), 138.00, 129.71, 128.81, 128.60 (phenyl),124.38 (s, =*C*H), 96.16 (s, *Cp*), 56.36 (s, PhCH_2N). IR (KBr)/cm^{-1}: ν_{sym}(CO) 1952 (vs), ν_{asym}(CO) 1874 (vs), I_{asym}/I_{sym} = 1.06 (predicted OC−Mo−CO angle 92°). Anal. Calcd for $C_{24}H_{21}BrN_2O_2Mo$: C, 52.86; H, 3.88; N, 5.14. Found: C, 53.19; H, 3.98; N, 5.09.

(η^5-C_5H_5)Mo(CO)$_2$(IMe^{n}Pr)Br (5). (Yield: 45% as a purple solid.) ^{1}H NMR (500 MHz, CD_3CN): δ (ppm) 7.21 (s, 2H, =CH_2), 5.58 (s, 5H, *Cp*), 4.03−3.97 (m,1H, $NCH_2CH_2CH_3$), 3.89−3.83 (m,1H, $NCH_2CH_2CH_3$), 3.63 (s, 3H, NCH_3), 1.79−1.75 (m, 2H, $NCH_2CH_2CH_3$), 0.94 (t, 3H, $NCH_2CH_2CH_3$, J = 6.95 Hz). ^{13}C NMR (125.77 MHz, CD_3CN): δ (ppm) 255.46 (s, Mo-*C*O), 251.47 (s, Mo-*C*O) 184.08 (s, N*C*N), 125.37 (s, =*C*H), 123.03 (s, =*C*H), 96.15 (s, *Cp*), 54.25 (s, $NCH_2CH_2CH_3$), 40.44 (s, NCH_3), 24.81 (s, $NCH_2CH_2CH_3$), 11.30 (s, $NCH_2CH_2CH_3$). IR (KBr)/cm^{-1}: ν_{sym}(CO) 1959 (vs), ν_{asym}(CO) 1858 (vs), I_{asym}/I_{sym} = 1.09 (predicted OC−Mo−CO angle 93°). Anal. Calcd for $C_{14}H_{17}BrN_2O_2Mo$: C, 39.93; H, 4.07; N, 6.65. Found: C, 39.71; H, 4.23; N, 6.15.

Synthesis of (η^5-C_5H_5)Mo(CO)$_2$(IMes)Br (3). Ag_2O (232 mg, 1 mmol) was added to a solution of 1,3-bis(2,4,6-trimethylphenyl)imidazolium bromide (340 mg, 1 mmol) in CH_2Cl_2 (15 mL). After refluxing for 8 h (exclusion of light), the reaction mixture was filtered through Celite. The filtrate was dried under vacuum and was dissolved in toluene (20 mL). $CpMo(CO)_3Br$ (0.6 mmol) was then added to the toluene solution. After refluxing for 40 min under stirring, the obtained purple solution was dried under vacuum and the purple solid was purified by column chromatography eluted by a mixture of hexane and ethyl acetate to give the product as a purple solid (yield: 75%). ^{1}H NMR (500 MHz, $CDCl_3$): δ (ppm) 7.14 (s, 2H, =C*H*), 7.05 (s, 2H, *m*-*H*-Mes), 7.00 (s, 2H, *m*-*H*-Mes), 4.71 (s, 5H, Cp), 2.38 (s, 6H, *p*-*Me*-Mes), 2.25 (s, 6H, o-*Me*-Mes), 2.17 (s, 6H, o-*Me*-Mes). ^{13}C NMR (125.77 MHz, $CDCl_3$): δ (ppm) 253.92 (s, Mo-*C*O), 246.60 (s, Mo-*C*O), 189.72 (s, N*C*N), 139.17 (s, *i*-*Mes*), 137.45 (s, *p*-*Mes*), 136.83 (s, *o*-*Mes*), 136.43 (s, *o*-*Mes*), 129.10 (s, *m*-*Mes*), 124.51(s, =*C*H), 94.75 (s, Cp), 21.06 (s, *p*-*Me*-Mes), 19.06 (s, *o*-Me-Mes). IR (KBr)/cm^{-1}: ν_{sym}(CO) 1956 (vs), ν_{asym}(CO) 1860 (vs), I_{asym}/I_{sym} = 1 (predicted OC−Mo−CO angle 90°). Anal. Calcd for $C_{28}H_{29}BrN_2O_2Mo$: C, 55.92; H, 4.86; N, 4.66. Found: C, 55.91; H, 4.72; N, 4.70.

Synthesis of (η^5-C_5H_5)Mo(CO)$_2$(IBz)Br (4a) and (η^5-C_5H_5)-Mo(CO)$_2$(IBz)Cl (4b) from $CpMo(CO)_2PPh_3Cl$. Ag_2O (232 mg, 1 mmol) was added to a solution of 1,3-dibenzylimidazolium

(19) Zoller, U. *Tetrahedron* **1988**, *24*, 7413.
(20) Dzyuba, S. V.; Bartsch, R. A. *Chem. Commun.* **2001**, 1466.
(21) Starikova, O. V.; Dolgushin, G. V.; Larina, L. I.; Ushakov, P. E.; Komarova, T. N.; Lopyrev, V. A. *Russ. J. Org. Chem.* **2003**, *39*, 1467.
(22) Shekaari, H.; Mousavi, S. S. *J. Chem. Thermodyn.* **2009**, *41*, 90.
(23) Lee, K. M.; Wang, H. M. J.; Lin, I. J. B. *J. Chem. Soc., Dalton Trans.* **2002**, 2852.
(24) Tanabe, Y.; Hanasaka, F.; Fujita, K.-I.; Yamaguchi, R. *Organometallics* **2007**, *26*, 4618.
(25) Newman, C. P.; Clarkson, G. J.; Rourke, J. P. *J. Organomet. Chem.* **2007**, *692*, 4962.
(26) Piper, T. S.; Wilkinson, G. *J. Inorg. Nucl. Chem.* **1956**, *3*, 104.
(27) Faller, J. W.; Anderson, A. S. *J. Am. Chem. Soc.* **1970**, *92*, 5852.
(28) Arduengo, A. J.; Krafczyk, R.; Schmutzler, R.; Craig, H. A.; Goerlich, J. R.; Marshall, W. J.; Unverzagt, M. *Tetrahedron* **1999**, *55*, 14523.

bromide (329 mg, 1 mmol) in CH_2Cl_2 (15 mL). After stirring at room temperature for 24 h upon exclusion of light, the reaction mixture was filtered through Celite. The filtrate was dried under vacuum and was dissolved in toluene (20 mL). $CpMo(CO)_2PPh_3Cl$ (309 mg, 0.6 mmol) was then added to the toluene solution. After refluxing for 30 min under stirring, the obtained purple solution was dried under vacuum and the purple solid was purified by column chromatography (hexane/ethyl acetate, 5:1). The two purple bands were collected as **4a** (yield: 98 mg, 30%) and **4b** (yield: 30 mg, 10%). The spectroscopic data of **4b**: ^{1}H NMR (500 MHz, CD_3CN): δ (ppm) 7.40−7.23 (br m, 10H, CH_2Ph), 7.08 (s, 2H, =C*H*), 5.43 (s, 5H, *Cp*), 5.35−5.19 (q, 4H, NCH_2Ph, J = 15.75 Hz). ^{13}C NMR (125.77 MHz, CD_3CN): δ (ppm) 256.20 (s, Mo-*C*O), 252.40 (s, Mo-*C*O) 188.79 (s, N*C*N), 138.17, 129.72, 128.78, 128.47 (phenyl), 124.36 (s, =*C*H), 96.60 (s, *Cp*), 55.95 (s, Ph*C*H$_2$N). IR (KBr)/cm^{-1}: ν_{sym}(CO) 1953 (vs), ν_{asym}(CO) 1872 (vs), I_{asym}/I_{sym} = 1.23 (predicted OC−Mo−CO angle 96°). Anal. Calcd for $C_{24}H_{21}ClN_2O_2Mo$: C, 57.56; H, 4.23; N, 5.59. Found: C, 57.56; H, 4.31; N, 5.61.

Synthesis of [(η^5-C_5H_5)Mo(CO)$_2$(IMes)(CH_3CN)][BF_4] (6). $AgBF_4$ (0.19 g, 1 mmol) was added to a solution of compound **3** (0.6 g, 1 mmol) in CH_3CN (20 mL). After stirring for 2 h at room temperature, the color of solution changed from purple to red. The reaction mixture was filtered through Celite, and the filtrate was dried under vacuum. The resulting dark red solid was recrystallized from acetonitrile and diethyl ether twice, yielding red crystals as the product (yield: 0.5 g, 80%). ^{1}H NMR (500 MHz, CD_3CN): δ (ppm) 7.49 (d, 2H, =C*H*), 7.14 (s, 2H, *m-H*-Mes), 7.09 (s, 2H, *m-H*-Mes), 4.94 (s, 5H, *Cp*), 2.36 (s, 6H, *p-Me*-Mes), 2.11 (s, 6H, *o-Me*-Mes), 2.02 (s, 6H, *o-Me*-Mes), 1.95 (s, 3H, CH_3CN). ^{13}C NMR (125.77 MHz, CD_3CN): δ (ppm) 248.54 (s, Mo-*C*O), 248.18 (s, Mo-*C*O), 183.91 (s, N*C*N), 140.71 (s, *i-Mes*), 137.41 (s, *p-Mes*), 136.74 (s, *o-Mes*), 136.71 (s, *o-Mes*), 130.15 (s, *m-Mes*), 129.91 (s, *m-Mes*), 127.11 (s, =*C*H), 95.48 (s, *Cp*), 20.92 (s, *p-Me*-Mes), 18.39 (s, *o-Me*-Mes), 18.26 (s, *o-Me*-Mes). IR (KBr)/cm^{-1}: ν_{sym}(CO) 1953 (vs), ν_{asym}(CO) 1870 (vs), I_{asym}/I_{sym} = 1.12 (predicted OC−Mo−CO angle 93°), ν(BF_4) 1038(vs). ESI-MS (in CH_3CN, m/z (%)): (M^+ − CH_3CN) = [(CpMo(CO)$_2$(IMes)]$^+$ = 523 (100). Anal. Calcd for $C_{30}H_{32}BF_4N_3O_2Mo$: C, 55.49; H, 4.97; N, 6.47. Found: C, 55.17; H, 5.05; N, 6.68.

Isolation and Characterization of [IMesH]$_2$[Mo_6O_{19}] from the Oxidation of Compound 3 by TBHP. Compound **3**, $CpMo(CO)_3$(IMes)Br (0.6 g, 1 mmol), was mixed with TBHP (5.0−6.0 M in decane) (1 mL, ca. 5.5 mmol) in CH_3CN (10 mL). After stirring for 12 h, the mixture was filtered and the filter cake was washed with CH_2Cl_2 and CH_3CN three times and dried under vacuum, giving a pale yellow solid (20 mg). ^{1}H NMR (500 MHz, d^6-DMSO): δ (ppm) 9.63 (m, 1H, NC*H*N), 8.26(d, 2H, =C*H*), 7.20 (s, 4H, *m-H*-Mes), 2.35 (s, 6H, *p-Me*-Mes), 2.12 (s, 12H, *o-Me*-Mes). ^{13}C NMR (125.77 MHz, DMSO): δ (ppm) 140.57 (s, N*C*HN), 138.44 (s, *i-Mes*), 134.24 (s, *p-Mes*), 130.93 (s, *o-Mes*), 129.31 (s, *m-Mes*), 124.76 (s, =*C*H), 20.57 (s, *p-Me*-Mes), 16.82 (s, *o*-Me-Mes). IR (KBr)/cm^{-1}: ν(Mo=O) 955.76 (vs), 800.05 (vs). Anal. Calcd for $C_{42}H_{50}N_4O_{19}Mo_6$: C, 33.84; H, 3.38; N, 3.76. Found: C, 32.44; H, 3.31; N, 3.43.

Synthesis of [$CpMoO_2$(IMes)][BF_4] (9). Compound **3** (300 mg, 0.5 mmol) and $AgBF_4$ (98 mg, 0.5 mmol) were dissolved in CH_3CN (15 mL). After stirring for 3 h at room temperature upon exclusion of light, the solution was filtered through Celite. TBHP (~5.5 M in decane over molecular sieves 4 Å) (2.5 mmol, 0.45 mL) was added to the filtrate, and the reaction mixture was stirred for 6 h at room temperature. After removing the solvent, the resulting yellow oil was washed with Et_2O and THF, giving a yellow solid as the final product (yield: 0.12 g, 40%). ^{1}H NMR (500 MHz, CD_3CN): δ (ppm) 7.86 (s, 2H, =C*H*), 7.12 (4H, m-*H*-Mes), 6.26 (s, 5H, *Cp*), 2.35 (s, 6H, *p-Me*-Mes), 2.07 (s, 12H, *o-Me*-Mes). ^{13}C NMR (125.77 MHz, CD_3CN): δ (ppm) 167.60 (s, N*C*N), 142.22 (s, *i-Mes*), 135.75 (s, *p-Mes* and *o-Mes*), 130.36 (s, *m-Mes*), 129.66(s, =*C*H), 114.69 (s, *Cp*), 21.02 (s, *p-Me*-Mes), 17.82 (s, *o-Me*-Mes). IR (KBr)/cm^{-1}: ν(Mo=O) 956 (s), 801 (s). ESI-MS (in CH_3CN, m/z (%)): M^+ = [($CpMoO_2$-(IMes)]$^+$ = 499 (100). Anal. Calcd for $C_{26}H_{29}BF_4MoN_2O_2$: C, 53.45; H, 5.00; N, 4.79. Found: C, 53.37; H, 5.44; N, 5.03.

Synthesis of $CpMoO_2Br$. $CpMoO_2Br$ was prepared by the reaction between $CpMo(CO)_3Br$ and TBHP according to the literature method for the synthesis of $CpMoO_2Cl$.[6a] ^{1}H NMR (500 MHz, CD_3CN): δ (ppm) = 6.76. ^{13}C NMR (125.77 MHz, CD_3CN): δ (ppm) = 115.6. IR (KBr)/cm^{-1}: ν(Mo=O) 909 (s), 801 (s).

X-ray Crystallography. Diffraction measurements were conducted at 100(2)−293(2) K on a Bruker AXS APEX CCD diffractometer by using Mo Kα radiation (λ = 0.71073 Å). The data were corrected for Lorentz and polarization effects with the SMART suite of programs and for absorption effects with SADABS.[29] Structure solutions and refinements were performed by using the programs SHELXS-97[30a] and SHELXL-97.[30b] The structures were solved by direct methods to locate the heavy atoms, followed by difference maps for the light non-hydrogen atoms. Anisotropic thermal parameters were refined for the rest of the non-hydrogen atoms. Hydrogen atoms were placed geometrically and refined isotropically.

Catalytic Reactions. Cyclooctene (0.4 g, 3.6 mmol), mesitylene (1 g, internal standard), and catalysts (1 mol %, 0.036 mmol) were added to the reaction vessel under an air atmosphere at 55 °C. The reaction was started by the addition of TBHP (5.0−6.0 M in *n*-decane; 7.2 mmol, 1.31 mL). The course of the reactions was monitored by quantitative GC analysis (Agilent 6890 Series GC instrument with a J&W DB-1 column). The samples were taken in regular time intervals, diluted with CH_2Cl_2, and treated with a catalytic amount of $MgSO_4$ and MnO_2 to remove water and to destroy the excess peroxide. The resulting slurry was filtered and the filtrate injected into the GC column. The conversion of cyclooctene and the formation of cyclooctene oxide were calculated from calibration curves (r^2 = 0.999) recorded prior to the reaction course.

Computational Details. All quantum chemical calculations have been performed using Gaussian 03.[16] The hybrid functional B3LYP[17,18] was employed. Geometry optimizations were performed using the default convergence criteria without any geometric constraints. The LANL2DZ ECP basis set[31] was applied for Mo, and the 6-31G+(d) basis set[32] was employed for the rest of the C, H, N, and O atoms. Characterization of the stationary points as minima or transition-state structures, as well as the determination of zero-point energies (ZPEs), was performed with frequency calculations.

Acknowledgment. We are grateful to the Ministry of Education (MOE) of Singapore Academic Research Fund (AcRF) Tier 1 Grant (WBS No. R-143-000-373-112). S.Y.L. also thanks National University of Singapore for the scholarship. K.W.H. acknowledges the support from KAUST baseline funding. We thank Ms. Geok Kheng Tan and Dr. Lip Lin Koh for determining the X-ray crystal structures.

Supporting Information Available: Crystallographic data in cif format and computational results are available free of charge via the Internet at http://pubs.acs.org.

(29) *SADABS: Area-Detection Absorption Correction*; Bruker AXS Inc.: Madison, WI, 1995.

(30) (a) Sheldrick, G. M. *SHELXS-97, Program for crystal structure solution*; University of Göttingen: Göttingen, Germany, 1997. (b) Sheldrick, G. M. *SHELXL-97, Program for crystal structure refinement*; University of Göttingen: Göttingen, Germany, 1997.

(31) (a) Hay, P. J.; Wadt, W. R. *J. Chem. Phys.* **1985**, *82*, 270. (b) Hay, P. J.; Wadt, W. R. *J. Chem. Phys.* **1985**, *82*, 299. (c) Wadt, W. R.; Hay, P. J. *J. Chem. Phys.* **1985**, *82*, 284.

(32) (a) Hehre, W. J.; Ditchfield, R.; Pople, J. A. *J. Chem. Phys.* **1972**, *56*, 2257. (b) Hariharan, P. C.; Pople, J. A. *Theor. Chim. Acta* **1973**, *28*, 213. (c) Clark, T.; Chandrasekhar, J.; Spitznagel, G. W.; Schleyer, P. v. R. *J. Comput. Chem.* **1983**, *4*, 294. (d) Rassolov, V. A.; Ratner, M. A.; Pople, J. A.; Redfern, P. C.; Curtiss, L. A. *J. Comput. Chem.* **2001**, *22*, 976.